Published in final edited form as:
Clin Cancer Res. 2011 August 1; 17(15): 4996–5004. doi:10.1158/1078-0432.CCR-10-3406.

Targeting GPCR-mediated p70S6K activity may improve head and neck cancer response to cetuximab

Neil E. Bhola[2], **Sufi M. Thomas**[1], **Maria Freilino**[1], **Sonali Joyce**[1], **Anirban Sahu**[1], **Jessica Maxwell**[1], **Athanassios Argiris**[3], **Raja Seethala**[4], and **Jennifer R. Grandis**[1,2]

[1] Department of Otolaryngology, University of Pittsburgh School of Medicine and University of Pittsburgh Cancer Institute, Pittsburgh, PA 15213, USA

[2] Department of Pharmacology and Chemical Biology, University of Pittsburgh School of Medicine and University of Pittsburgh Cancer Institute, Pittsburgh, PA 15213, USA

[3] Department of Medicine, University of Pittsburgh School of Medicine and University of Pittsburgh Cancer Institute, Pittsburgh, PA 15213, USA

[4] Department of Pathology, University of Pittsburgh School of Medicine and University of Pittsburgh Cancer Institute, Pittsburgh, PA 15213, USA

Abstract

Purpose—EGFR overexpression is correlated with decreased survival in head and neck cancer (HNC) where the addition of EGFR inhibition to standard chemoradiation approaches has improved treatment responses. However, the basis for the limited efficacy of EGFR inhibitors in HNC is incompletely understood. G-protein-coupled receptors (GPCRs) have been shown to be overexpressed in HNC where GPCR activation induces HNC growth via both EGFR-dependent and independent pathways. We hypothesized that targeting GPCR-induced EGFR-independent signaling would improve the efficacy of EGFR inhibition.

Experimental Design—Using a high-throughput phospho-proteome array, we identified proteins that were phosphorylated in HNC cells where EGFR expression was downmodulated by RNAi in the presence or absence of a GPCR ligand. We confirmed the findings from the array by Western blotting followed by *in vitro* and *in vivo* phenotypic assays.

Results—p70S6K phosphorylation was elevated approximately 6-fold in EGFR siRNA transfected cells treated with a GPCR ligand. In addition to RNAi-mediated EGFR downmodulation, GPCR-mediated phosphorylation of p70S6K was modestly increased by the FDA-approved EGFR inhibitor cetuximab. Biopsies from cetuximab treated patients also displayed increased phospho-p70S6K staining compared to pre-treatment biopsies. HNC cells were growth inhibited by both genetic and pharmacological p70S6K targeting strategies. Furthermore, p70S6K targeting in combination with cetuximab resulted in enhanced anti-tumor effects in both *in vitro* and *in vivo* HNC models.

Conclusions—These results indicate that increased phosphorylation of p70S6K in cetuximab-treated patients may be due to increased GPCR signaling. Therefore, the addition of p70S6K targeting strategies may improve treatment responses to EGFR inhibition.

Corresponding Author: Jennifer Rubin Grandis, Suite 500 Eye and Ear Institute, 203 Lothrop Street, University of Pittsburgh, Pittsburgh, PA 15213, Telephone number: 412-647-5280, Fax number: 412-647-0108, grandisjr@upmc.edu.

INTRODUCTION

Head and neck squamous cell carcinoma (HNC) is characterized by overexpression of the Epidermal Growth Factor Receptor (EGFR). Increased expression of EGFR in HNC has been correlated with decreased patient survival, regardless of primary therapy (1). The addition of the EGFR monoclonal antibody cetuximab (C225, ™ Erbitux) to radiation therapy improved survival leading to the FDA approval of this agent for HNC in 2006 (2). However, only a subset of HNC patients will experience a clinical response to cetuximab when administered as a primary treatment approach or in the setting of recurrent or metastatic disease (3). To date, no consistent association between response to EGFR inhibition and baseline expression of a specific biomarker, including EGFR, has been demonstrated. In addition, there is a paucity of studies analyzing post-treatment tumors from patients treated with cetuximab, so that the effects of EGFR inhibitors on other signaling pathways *in vivo* are largely unexplored.

G-protein-coupled receptors (GPCRs) are seven transmembrane receptors that mediate cell growth, motility and differentiation via stimulation by cognate agonists (4). The GPCR, bradykinin receptor 2 (B2R), which stimulates the upregulation of cyclooxygenase 2 (COX-2) and its downstream effector PGE2, another GPCR ligand, is overexpressed in HNC (5, 6). We and others have shown that GPCR ligands including PGE2, BK, GRP and lysophosphatidic acid (LPA) mediate HNC proliferation and invasion via the autocrine release of EGFR ligands and the consequent activation of EGFR (7–9). Furthermore, combined inhibition of GPCRs and EGFR displayed enhanced anti-tumor effects, indicating that GPCRs can induce EGFR-independent pathways in addition to transactivation of EGFR (9, 10). Identification of the proteins induced in the absence of EGFR, or in the setting of EGFR blockade, may reveal new therapeutic targets, which can be inhibited to augment clinical responses in combination with cetuximab.

The present study was carried out to elucidate “druggable” targets that contribute to GPCR-mediated HNC growth when EGFR is downregulated or inhibited. We used an antibody microarray to identify proteins that were activated by GPCRs under EGFR downmodulated conditions. We then targeted the activated pathway using genetic and pharmacologic approaches, alone and in combination with EGFR inhibitors, in HNC preclinical models *in vitro* and *in vivo*.

MATERIALS AND METHODS

Cell lines

All HNC cell lines (PCI-37A, 1483, UM-22B, CAL133 and 686LN) were of human origin. 1483 cells were derived from an oropharyngeal tumor, UM-22B cell line was derived from metastatic lymph nodes and PCI-37A was from a primary tumor in the epiglottis (11). CAL133 were derived from oral squamous cell carcinoma cells (12) were a kind gift from Dr Gerard Milano (Centre Antoine-Lacassagne, Nice, France). 686LN cell line was derived from the lymph node metastasis of a patient with oral squamous cell carcinoma and was a kind gift from Dr Georgia Chen (Emory University, Atlanta, GA). Cells were maintained in DMEM with 10% heat-inactivated FCS (Invitrogen, Carlsbad, CA) at 37°C with 5% CO_2.

Reagents

Epidermal growth factor (EGF), and Prostaglandin E2 (PGE2) were obtained from Calbiochem (San Diego, CA). Bradykinin was obtained from Bachem (Torrance, CA). RAD001 (Everolimus) was provided by Novartis (Basel, Switzerland) and C225 (cetuximab, ™ Erbitux) was obtained from the University of Pittsburgh Cancer Institute pharmacy.

Phospho-protein antibody array

Phospho-protein arrays were obtained from FullMoon Biosystems (Sunnyvale, CA). PCI-37A cells were seeded in four 10 cm culture dishes; 1) nontargeting control (NTC) siRNA plus vehicle, 2) NTC siRNA plus PGE2, 3)EGFR siRNA plus vehicle, 4) EGFR siRNA plus PGE2. Cells were transiently transfected with NTC siRNA or EGFR siRNA, serum-starved for 72 hours and treated with vehicle or 10 nM PGE2. Cells were lysed with Extraction Buffer provided as described according to manufacturer's instructions. Protein samples were biotinylated using Biotin reagent dissolved in N,N-Dimethylformamide. 10 μl of protein sample was mixed with 40 μl of Labeling Buffer followed by addition of Biotin/DMF reagent at a 1:7 ratio. Biotin-labeled protein samples were conjugated to the cancer/apoptosis phospho-antibody array. Antibody array slides were incubated with Blocking Solution provided on a rotating shaker at room temperature. Slides were then rinsed three times in water and allowed to dry. Protein coupling mix was added over the array slide and incubated at 4°C overnight. Slides were washed twice for 10 minutes each with 1X Wash Solution. Cy3-streptavidin solution was then added to the slides for 60 minutes at room temperature with shaking. Slides were scanned using the GenePix 4300 Array Scanner. Fold-change in intensities from six replicates between PGE2-treated NTC siRNA and PGE2-treated EGFR siRNA cells was calculated and tabulated (Supplementary Table 1).

Immunoblotting

Cells were lysed with lysis buffer and quantitated as described previously. Lysates were resolved by 8% or 10% SDS-PAGE. After being transferred onto a nitrocellulose membrane, the membrane was blocked in 5% milk and blotted with various primary antibodies in 5% milk dissolved in TBST solution [0.6% dry milk powder, 0.9% NaCl, 0.5% Tween 20, and 50mmol/L Tris (pH 7.4)]. After washing three times with TBST solution, the membrane was incubated with the secondary antibody (goat antirabbit/mouse IgG-horseradish peroxidase conjugate; Bio-Rad Laboratories) for 1 hour and washed three times for 10 minutes. Membranes were developed with Luminol Reagent (Santa Cruz Biotechnology) by autoradiography. Blots were stripped in Restore Western Blot Stripping buffer (Pierce, Rockford, IL) for 25 minutes at room temperature, blocked for 1 hour, and reprobed with primary antibodies.

RNA interference studies

Silencing RNA oligonucleotides targeting EGFR, p70S6K, were obtained from Dharmacon (Lafayette, CO). EGFR siRNA was designed to target the following sequence: 5′ – CUCUGGAGGAAAAGAAA-3′. P70S6K siRNA was designed to target the following sequence: 5′-CCAAGGUCAUGUGAAACUA-3′. 2×10^6 HNC cells were seeded in 10 cm plates and allowed to incubate overnight at 37°C. Cells were transfected with siRNA using Lipofectamine 2000 (Invitrogen) according to the manufacturer's instructions. CAL133 cells were infected with lentiviral particles encoding p70S6K shRNA (UPCI Vector Core Facility, Pittsburgh, PA), cultured and selected with puromycin for 2 weeks. Clones were selected with puromycin, cultured and verified for protein knockdown of p70S6K.

Proliferation assays

HNC cells were seeded and incubated overnight at 37°C. Cells were treated with pharmacologic inhibitors or transfected with siRNA for different time points. For experiments involving p70S6K siRNA alone, 3-(4,5-dimethylthiazol-2-yl)-2,5-diphenyltetrazolium bromide (MTT) assay was performed as described previously(10). For subsequent experiments involving cytostatic inhibitors cetuximab and RAD001, we observed no effect with MTT assay. Subsequent testing of different cell viability assays was performed and growth-inhibitory experiments involving cetuximab and RAD001 were

determined using the more sensitive fluorimetric resazurin-based Cell Titer Glo Assay (Promega, WI) according to manufacturer's instructions. Cells were read using a Victor3 multilabel counter at 560ex/590em wavelengths. For BK-treated experiments, cells were trypsinized and stained with trypan blue solution before being transferred to a hemocytometer and viable cells were counted.

Matrigel invasion assays

In vitro invasion assays were performed in the growth-factor reduced Matrigel-coated Transwell chambers (BD Biosciences, San Jose, CA). 1483 cells were plated in a 6-well plate. Twenty-four hours later, 4 wells were treated with vehicle, C225, RAD001, and C225 and RAD001 in serum-free media for 48 hours. For p70S6K siRNA studies, cells were seeded and transfected with control or p70S6K siRNA for 48 hours. Cells were trypsinized, counted and plated in serum-free media into the Transwell chambers. For p70S6K siRNA experiments, cells used for invasion assay were plated in Cell -Titer Glo assay to determine survival. The lower well contained 10% serum-containing media and cells were allowed to invade for 24 hours at 37°C and 5% CO2. The cells on the insert were removed by gently wiping with a cotton swab. Cells on the reverse side of the insert were fixed and stained with Hema3 Solution (Fisher Scientifics, Hampton, NH). Invading cells in 5 representative fields were counted at 400X magnification using light microscopy. The percentage invasion was calculated and normalized to cell survival in the p70S6K siRNA experiments.

Xenograft experiments

All animal procedures and care was done under the guidelines instituted by the Institutional Animal Care and Use Committee at the University of Pittsburgh. Athymic nude mice were injected subcutaneously with 2×10^6 1483 or UM-22B cells in the right flank. Tumor-bearing mice were randomized into four groups; Vehicle (saline), C225, RAD001, or C225 plus RAD001. C225 was administered by IP injection at a dose of 0.8mg/mouse twice weekly while RAD001 was administered 5 days a week at a dose of 5mg/kg over a four-week period. RAD001 was provided as a 2% microemulsion which was dissolved in fresh 5% glucose daily before administration. For UM-22B xenografts, mice were treated with 5mg/kg placebo or RAD001 daily for 12 days immediately following randomization and the first tumor measurement.

Immunohistochemical analysis and construction of tissue microarrays

Tumor biopsies were obtained from HNC patients under a protocol approved by the Institutional Review Board at the University of Pittsburgh (IRB#991206). Informed consent was obtained from all subjects. Paraffin 'donor' blocks which contained the highest percentage of tumor were selected for each case by one of the authors (RRS). Using a manual tissue arrayer (MTA-1, Beecher Instruments, (Sun Prairie, WI) 1.0 mm cores were transferred from each donor block to a blank recipient paraffin block and arrayed in duplicate along with normal tonsillar controls. The newly constructed array block was then warmed to 35–37°C for 10 minutes to allow annealing of donor cores to the paraffin wax of the recipient block and minimize core loss. Donor cores ranged from 2–4 mm in length. Immunohistochemistry (IHC) was performed on formalin-fixed paraffin-embedded TMA sections using antibodies against phospho-p70S6K T421/S424 (1:75 dilution, 1:75 overnight 4°C incubation, Santa Cruz Biotechnology, Santa Cruz, CA). Antigen retrieval was performed for 15 minutes in 0.01M citrate buffer. TMAs were blocked and stained with primary antibodies. Following three 5 minute washes, TMAs were incubated with biotinylated anti-rabbit secondary followed by ABC complex. Signal was developed with DAB substrate, modestly counterstained with hematoxylin and slides were analyzed microscopically. Immunohistochemical staining was assessed semi-quantitatively for each core. The percentage of immunoreactive cells was recorded and rounded to the nearest 10

percentile. Additionally, intensity was scored as follows: 0 (none), 1+ (weak), 2+ (moderate) 3+ (strong). A composite score was derived from the product of the percentage and intensity of staining. The scores across replicate cores on slides were averaged. The average composite score for both antibodies were graphed using GraphPad Prism Software.

Statistics

The differences between treatment groups in biochemical, growth and invasion assays were tested with the two-tailed Student's t-test. The differences between treatment groups in xenograft experiments were tested with the exact Wilcoxon Mann Whitney 1-sided test. $P < 0.05$ was considered to be statistically significant.

RESULTS

GPCR ligands activate p70S6K in the absence of EGFR

We previously reported that in the presence of EGFR inhibition, the GPCR ligands prostaglandin E2 (PGE2) and bradykinin (BK) induced Erk activation (9, 10). We therefore wanted to identify GPCR-induced "druggable" pathways that mediated EGFR-independent growth in HNC. We performed a phospho-protein antibody array to identify phosphorylated proteins that were induced in HNC cells transfected with EGFR siRNA compared with control siRNA in the setting of PGE2 stimulation. We firstly verified the efficacy of EGFR siRNA and showed that it down modulated EGFR expression 72 hours post-transfection (Supplemental Figure 1). There was a 2-fold or greater increase in phosphorylation of 5 of the 155 proteins assessed in the array induced by EGFR knockdown/PGE2 treatment (Table 1). Of the five proteins identified, expression of phosphorylated p70S6K (Ser 424) was induced to the greatest degree (5.6-fold). We confirmed the increased activation of p70S6K in samples used in the array by immunoblotting for the Thr389 site of p70S6K (Supplemental Figure 1). We also confirmed increased expression of phosphorylated forms of PKCδ and MAPK. Interestingly, p70S6K phosphorylation was significantly induced in the EGFR siRNA transfected cells compared to control siRNA transfected cells in the absence of exogenous stimulation with PGE2. This observation was investigated separately in our laboratory. To extend the observations to other HNC models and GPCR ligands, we examined the effect of EGFR downmodulation on GPCR-mediated p70S6K phosphorylation and found that bradykinin (BK) induced a 4-fold and 2.5-fold induction of p70S6K phosphorylation in UM-22B and 1483 cells following EGFR siRNA transfection respectively (Figures 1A and 1B; P=0.01, P=0.03). Similar to the observations from the lysates used in the array (Supplemental Figure 1), we observed increases (3- and 2-fold respectively) in p70S6K phosphorylation by EGFR knockdown even without GPCR stimulation in UM-22B and 1483, respectively. These results suggest that p70S6K may be an EGFR-independent molecular target that is activated in the setting of EGFR blockade and further enhanced by GPCR signaling.

BK-induced p70S6K phosphorylation is modestly induced in the presence of the EGFR inhibitor cetuximab

We previously reported that PGE2 and BK activated MAPK activation in the presence of the EGFR TKI AG1478 (9). To determine the pharmacologic significance of the effects observed with EGFR siRNA, we chose to investigate p70S6K signaling in the presence of the FDA-approved EGFR inhibitor cetuximab (C225). Cetuximab's mode of action involves neutralization of the ligand-binding domain and internalization of EGFR. As shown in Figure 1C, BK-mediated induction of phosphorylated p70S6K was modestly increased in the presence of cetuximab. EGF stimulation was used as a control for C225 efficacy, as EGF-induced p70S6K phosphorylation was abrogated by C225 treatment (Figure 1C and

Supplemental Figure 2). These results indicate that BK induces p70S6K phosphorylation independently of EGFR.

Post-cetuximab HNC biopsies display elevated p70S6K phosphorylation levels

Cetuximab (C225, Erbitux™) is a monoclonal antibody that has been reported to mediate its action by downregulating EGFR membrane expression and is FDA-approved for the treatment of HNC. The effect of cetuximab on phosphorylated p70S6K has not been reported in human cancer. To determine the role of p70S6K activation in the setting of cetuximab treatment we evaluated a tissue microarray containing samples obtained before and/or after the administration of cetuximab in a cohort of HNC patients treated at the University of Pittsburgh. Tumor tissue was obtained from a total of 19 patients including 12 patients with tissue biopsies prior to cetuximab treatment, 5 patients with tissue biopsies after progression on cetuximab and 2 patients with paired tumor sample biopsies prior to and after cetuximab exposure. All patients were previously cetuximab naïve. Patient characteristics are listed in Table 2. Immunohistochemical staining of the TMA with phospho-p70S6K (Thr421/Ser424) was performed and the composite scores were calculated (incorporating both the intensity of staining and the % of cells that stained positively). In the seven tumor samples obtained following progression after cetuximab treatment, expression of phospho-p70S6K was elevated 2-fold compared to levels in the fifteen tumors biopsies obtained prior to cetuximab administration (Figure 2A), including the two paired biopsies (Figure 2B). Although there were only 2 patients with paired tumor tissue for analysis, both progressed on cetuximab therapy suggesting that increased expression of phosphorylated p70S6K may be associated with poor response to cetuximab. The observations made in these limited patient samples suggest that p70S6K may be a possible therapeutic target that can be exploited to improve responses to EGFR targeted therapy.

Targeting p70S6K decreases HNC growth *in vitro* and *in vivo*

We previously reported that combination of BK and PGE2 antagonists with EGFR inhibitors resulted in improved anti-proliferative and anti-invasive effects *in vitro* (9). Therefore, we wanted to determine if p70S6K inhibition in combination with C225 would lead to enhanced anti-tumor effects compared with each agents administered alone. First, we targeted p70S6K using both RNAi and the pharmacological inhibitor RAD001. Small interfering RNA completely abrogated the protein expression of p70S6K in both UM-22B and 1483 cell lines 72 hours post-transfection in conjunction with significant growth inhibition compared to control siRNA-treated cells ($P<0.001$; Figure 3A and B). In addition to siRNA, we also showed that p70S6K shRNA decreased p70S6K expression and HNC growth (Supplemental Figure 3). The mTOR inhibitor RAD001 (everolimus) was previously reported to abrogate p70S6K phosphorylation in ovarian cancer cells (13). We observed that 10 nM and 100 nM of RAD001 completely abolished p70S6K phosphorylation in UM-22B and 1483 cells respectively (Figure 3C). Next, we determined the IC_{50} values for RAD001 on 1483 and UM-22B cells in vitro. In Figure 3D, RAD001 had a cytostatic effect and only induced 50% cell death at a concentration of 14μM. At 10nM and 100nM concentrations, there was an approximate 20% decrease in HNC survival. To test the effects of p70S6K inhibition on tumor growth *in vivo*, HNC xenograft-bearing mice were treated with RAD001 (5 mg/kg daily) in conjunction with tumor volume determinations. As shown in Figure 3E, RAD001 significantly decreased HNC tumor growth *in vivo* compared to placebo ($P=0.001$).

Targeting p70S6K enhances cetuximab-mediated anti-tumor effects

Having established that p70S6K inhibition was associated with anti-proliferative effects, we next sought to determine the efficacy of combining p70S6K inhibition with EGFR blockade. We treated control and p70S6K siRNA-transfected HNC cells with the EGFR inhibitor cetuximab followed by cell viability determinations. Compared to cetuximab or p70S6K

siRNA alone, we observed that downregulation of p70S6K increased the effects of cetuximab on HNC growth in both HNC cell lines tested ($P<0.05$; Figure 4A). Similar effects were observed with p70S6K shRNA cells treated with cetuximab (Supplemental Figures 3 and 4). In the presence of BK which has been previously shown to increase EGFR ligand production (9), the combination of cetuximab plus RAD001 decreased HNC growth to a greater degree compared with cetuximab or RAD001 alone (Figure 4B; $P < 0.05$). In addition to proliferation, we investigated the combined effects of cetuximab plus RAD001 on HNC invasion. Cetuximab or RAD001 alone decreased HNC invasion by 50%. However, an enhanced 20% reduction of invasion was observed using a combination of cetuximab plus RAD001 (Figure 4C; $P=0.02$). Cetuximab also enhanced the anti-invasive effects in p70S6K siRNA-transfected cells (Supplemental Figure 5). Next, we treated HNC tumor-bearing mice with sub-therapeutic doses of cetuximab (0.8 mg C225 i.p twice weekly), RAD001 (5 mg/kg p.o five days/week), or combined treatment with cetuximab plus RAD001, or vehicle control. After 28 days we observed that the combination of low dose cetuximab plus RAD001 significantly decreased tumor growth compared to cetuximab alone (Figure 4D; $P=0.03$). These observations demonstrate that targeting p70S6K activation can increase the efficacy of cetuximab treatment in HNC.

DISCUSSION

The monoclonal EGFR antibody cetuximab (C225/Erbitux™) was FDA-approved for the treatment of primary HNC in combination with radiation in 2006, making it the first new drug for this cancer in over 45 years (2). Despite widespread EGFR expression, cetuximab is only effective in a subset of HNC patients. We previously reported that GPCR ligands can transactivate EGFR via autocrine release of EGFR ligands (9, 14). In addition, GPCR ligands can activate the mitogenic MAPK pathway in the presence of EGFR inhibitors and combined targeting of individual GPCRs and EGFR resulted in enhanced survival in the presence of GPCR ligands in the presence of GPCR ligand inhibition (9, 10). In this study, we showed that GPCR ligand BK can enhance the phosphorylation of p70S6K in the presence of EGFR siRNA or cetuximab. In addition, we observed combined treatment with cetuximab and RAD001 improves anti-tumor response in both *in vitro* and *in vivo* HNC models.

GPCRs have been previously linked to the activation of p70S6K in different benign and malignant cell types. In bladder cancer, the GPCR ligand carbachol was shown to activate p70S6K in the presence of the EGFR TKI AG1478 (15). In smooth muscle airway cells, thrombin and EGF were reported to synergistically activate p70S6K (16). In addition, we identified that p70S6K phosphorylation was additively decreased by combined treatment with a GRPR inhibitor and EGFR TKI using RPPA analysis (10). In the present study, we show for the first time that in the presence of EGFR downmodulating agents including cetuximab, GPCR ligands can induce p70S6K phosphorylation. We also observed that even in the absence of GPCR ligands, EGFR downmodulation results in increased p70S6K phosphorylation alone. Furthermore, the increased expression of phosphorylated p70S6K in post-cetuximab treated biopsies support p70S6K as plausible therapeutic target to overcome de novo and acquired resistance to EGFR inhibition.

While studies to date have not identified p70S6K activation as a feedback mechanism in response to EGFR downmodulation, several reports demonstrate that inhibition of EGFR results in activation of the insulin growth factor receptor pathway, which signals via the PI3K/Akt/p70S6K pathway (17, 18). IGF1R downmodulation has been shown to augment EGFR signaling. Furthermore, our antibody array showed that phospho-IRS (Ser312) was increased 2-fold in EGFR siRNA transfected cells (Table 1) and it has been reported that mTOR/p70S6K regulates the phosphorylation at this site in the presence of insulin (19).

Therefore, it is possible that EGFR downmodulation in HNC leads to increased p70S6K phosphorylation, at least in part, via increased insulin signaling.

The effects of mTOR inhibitors have been shown to be promising in preclinical HNC models (20, 21). However, rapalogs are allosteric inhibitors and their activity results in a feedback loop that induces Akt phosphorylation (22). However, dual PI3K/mTOR inhibitors(23) may be more potent in overcoming the limited clinical efficacy of cetuximab. Although the combination of C225 and RAD001 did not result in tumor regression, this may be due to use of the subtherapeutic concentrations of cetuximab used. Therefore, it is possible that a combination of therapeutic doses of cetuximab and RAD001 will be more potent and result in tumor regression.

It is also important to note that RAD001 lacks specificity and also inhibits phoshporylation of 4EBP1 so it is not possible to distinguish precisely which target is most important using this rapalog. The results of the present study provide a biological basis for the ongoing clinical trial combining cetuximab and RAD001 in HNC patients (http://clinicaltrials.gov/ct2/show/NCT01009346). Since GPCR ligands including BK and PGE2 in HNC are ubiquitous in the tumor microenvironment, p70S6K represents a promising therapeutic target, particularly in combination with EGFR blockade.

Supplementary Material

Refer to Web version on PubMed Central for supplementary material.

References

1. Grandis JR, Melhem MF, Gooding WE, Day R, Holst VA, Wagener MM, Drenning SD, Tweardy DJ. Levels of TGF-alpha and EGFR protein in head and neck squamous cell carcinoma and patient survival. J Natl Cancer Inst. 1998 June 3; 90(11):824–32. [PubMed: 9625170]
2. Bonner JA, Harari PM, Giralt J, Azarnia N, Shin DM, Cohen RB, Jones CU, Sur R, Raben D, Jassem J, Ove R, Kies MS, Baselga J, Youssoufian H, Amellal N, Rowinsky EK, Ang KK. Radiotherapy plus Cetuximab for Squamous-Cell Carcinoma of the Head and Neck. N Engl J Med. 2006 February 9; 354(6):567–78. [PubMed: 16467544]
3. Vermorken JB, Mesia R, Rivera F, Remenar E, Kawecki A, Rottey S, Erfan J, Zabolotnyy D, Kienzer H-R, Cupissol D, Peyrade F, Benasso M, Vynnychenko I, De Raucourt D, Bokemeyer C, Schueler A, Amellal N, Hitt R. Platinum-Based Chemotherapy plus Cetuximab in Head and Neck Cancer. N Engl J Med. 2008 September 11; 359(11):1116–27. [PubMed: 18784101]
4. Dorsam R, Gutkind S. G-protein-coupled receptors and cancer. Nat Rev Canc. 2007; 7:79–94.
5. Jung T, Berlinger N, Juhn S. Prostaglandins in squamous cell carcinoma of the head and neck: a preliminary study. Laryngoscope. 1985; 95:307–12. [PubMed: 3919231]
6. Zhang W, Bhola N, Kalyankrishna S, Gooding W, Hunt J, Seethala R, Grandis JR, Siegfried JM. Kinin B2 Receptor Mediates Induction of Cyclooxygenase-2 and Is Overexpressed in Head and Neck Squamous Cell Carcinomas. Mol Cancer Res. 2008 December 1; 6(12):1946–56. [PubMed: 19074839]
7. Gschwind A, Prenzel N, Ullrich A. Lysophosphatidic Acid-induced Squamous Cell Carcinoma Cell Proliferation and Motility Involves Epidermal Growth Factor Receptor Signal Transactivation. Cancer Res. 2002 November 1; 62(21):6329–36. [PubMed: 12414665]
8. Lango MN, Dyer KF, Lui VWY, Gooding WE, Gubish C, Siegfried JM, Grandis JR. Gastrin-Releasing Peptide Receptor-Mediated Autocrine Growth in Squamous Cell Carcinoma of the Head and Neck. J Natl Cancer Inst. 2002 March 6; 94(5):375–83. [PubMed: 11880476]
9. Thomas SM, Bhola NE, Zhang Q, Contrucci SC, Wentzel AL, Freilino ML, Gooding WE, Siegfried JM, Chan DC, Grandis JR. Cross-talk between G Protein-Coupled Receptor and Epidermal Growth Factor Receptor Signaling Pathways Contributes to Growth and Invasion of Head and Neck Squamous Cell Carcinoma. Cancer Res. 2006 December 15; 66(24):11831–9. [PubMed: 17178880]

10. Zhang Q, Bhola NE, Lui VWY, Siwak DR, Thomas SM, Gubish CT, Siegfried JM, Mills GB, Shin D, Grandis JR. Antitumor mechanisms of combined gastrin-releasing peptide receptor and epidermal growth factor receptor targeting in head and neck cancer. Mol Cancer Ther. 2007 April 1; 6(4):1414–24. [PubMed: 17431120]
11. Sacks PG, Parnes SM, Gallick GE, Mansouri Z, Lichtner R, Satya-Prakash KL, Pathak S, Parsons DF. Establishment and Characterization of Two New Squamous Cell Carcinoma Cell Lines Derived from Tumors of the Head and Neck. Cancer Res. 1988 May 15; 48(10):2858–66. [PubMed: 2452013]
12. Gioanni J, Fischel J-L, Lambert J-C, Demard F, Mazeau C, Zanghellini E, Ettore F, Formento P, Chauvel P, Lalanne C-M, Courdi A. Two new human tumor cell lines derived from squamous cell carcinomas of the tongue: Establishment, characterization and response to cytotoxic treatment. European Journal of Cancer and Clinical Oncology. 1988; 24(9):1445–55.
13. Mabuchi S, Altomare DA, Cheung M, Zhang L, Poulikakos PI, Hensley HH, Schilder RJ, Ozols RF, Testa JR. RAD001 Inhibits Human Ovarian Cancer Cell Proliferation, Enhances Cisplatin-Induced Apoptosis, and Prolongs Survival in an Ovarian Cancer Model. Clin Cancer Res. 2007 July 15; 13(14):4261–70. [PubMed: 17634556]
14. Zhang Q, Thomas SM, Xi S, Smithgall TE, Siegfried JM, Kamens J, Gooding WE, Grandis JR. Src Family Kinases Mediate Epidermal Growth Factor Receptor Ligand Cleavage, Proliferation, and Invasion of Head and Neck Cancer Cells. Cancer Res. 2004 September 1; 64(17):6166–73. [PubMed: 15342401]
15. Jiang X, Sinnett-Smith J, Rozengurt E. Carbachol induces p70S6K1 activation through an ERK-dependent but Akt-independent pathway in human colonic epithelial cells. Biochemical and Biophysical Research Communications. 2009; 387(3):521–4. [PubMed: 19615971]
16. Billington CK, Kong KC, Bhattacharyya R, Wedegaertner PB, Panettieri RA, Chan TO, Penn RB. Cooperative Regulation of p70S6 Kinase by Receptor Tyrosine Kinases and G Protein-Coupled Receptors Augments Airway Smooth Muscle Growth. Biochemistry. 2005 November 8; 44(44): 14595–605. [PubMed: 16262259]
17. Chakravarti A, Loeffler JS, Dyson NJ. Insulin-like Growth Factor Receptor I Mediates Resistance to Anti-Epidermal Growth Factor Receptor Therapy in Primary Human Glioblastoma Cells through Continued Activation of Phosphoinositide 3-Kinase Signaling. Cancer Res. 2002 January 1; 62(1):200–7. [PubMed: 11782378]
18. Jones HE, Goddard L, Gee JMW, Hiscox S, Rubini M, Barrow D, Knowlden JM, Williams S, Wakeling AE, Nicholson RI. Insulin-like growth factor-I receptor signalling and acquired resistance to gefitinib (ZD1839; Iressa) in human breast and prostate cancer cells. Endocr Relat Cancer. 2004 December 1; 11(4):793–814. [PubMed: 15613453]
19. Carlson CJ, White MF, Rondinone CM. Mammalian target of rapamycin regulates IRS-1 serine 307 phosphorylation. Biochemical and Biophysical Research Communications. 2004; 316(2):533–9. [PubMed: 15020250]
20. Aissat N, Le Tourneau C, Ghoul A, Serova M, Bieche I, Lokiec F, Raymond E, Faivre S. Antiproliferative effects of rapamycin as a single agent and in combination with carboplatin and paclitaxel in head and neck cancer cell lines. Cancer Chemotherapy and Pharmacology. 2008; 62(2):305–13. [PubMed: 17912526]
21. Czerninski R, Amornphimoltham P, Patel V, Molinolo AA, Gutkind JS. Targeting Mammalian Target of Rapamycin by Rapamycin Prevents Tumor Progression in an Oral-Specific Chemical Carcinogenesis Model. Cancer Prev Res. 2009 January 1; 2(1):27–36.
22. O'Reilly KE, Rojo F, She QB, Solit D, Mills GB, Smith D, Lane H, Hofmann F, Hicklin DJ, Ludwig DL, Baselga J, Rosen N. mTOR inhibition induces upstream receptor tyrosine kinase signaling and activates Akt. Cancer Res. 2006 Feb 1; 66(3):1500–8. [PubMed: 16452206]
23. Zhang Y-J, Duan Y, Zheng XFS. Targeting the mTOR kinase domain: the second generation of mTOR inhibitors. Drug Discovery Today. 2011; 16(7-8):325–31. [PubMed: 21333749]

Translational Relevance

EGFR overexpression is correlated with poor prognosis in head and neck cancer (HNC) where efforts to date to target EGFR have been associated with limited clinical responses. Identification of alternative signaling mechanisms that promote tumor survival in the presence of EGFR blockade may identify new targets that when inhibited, can improve responses to anti-EGFR strategies. Here we show that G-protein-coupled receptors (GPCRs) activate p70S6K as a consequence of EGFR targeting. Furthermore, biopsies from cetuximab treated patients displayed elevated p70S6K phosphorylation. Combined inhibition of p70S6K and EGFR was associated with improved anti-tumor effects in HNC preclinical models. These results indicate that inhibition of EGFR is associated with activation of collateral signaling pathways including p70S6K, which when targeted, can improve response to EGFR inhibitors. Clinical trials to test the efficacy of combined EGFR and p70S6K targeting in cancer patients are underway.

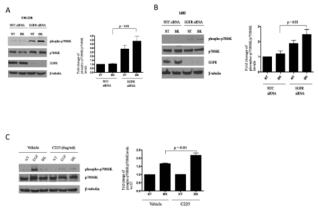

Figure 1. BK induces p70S6K phosphorylation in presence of EGFR targeting agents

(A) UM-22B and (B) 1483 cells were transiently transfected with EGFR siRNA, serum-starved for 72 hours and stimulated with either vehicle or BK (10 nM) for 10 minutes. Lysates were collected and resolved by SDS-PAGE for phospho-p70S6K (Thr389). Denistometry represents the results of 3 independent experiments (For UM-22B, P=0.01; 1483, P=0.03). (C) UM-22B cells were serum-starved for 72 hours and then pre-incubated with 6μg/ml C225 for 2 hours. Cells were then treated with either vehicle or 10nM BK for 10 minutes. Lysates were collected and resolved by SDS-PAGE for phospho-p70S6K (Thr389). Denistometry represents the results of 3 independent experiments (P = 0.03).

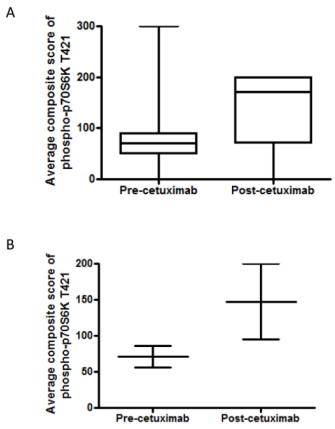

Figure 2. HNC patients display increased p70S6K phosphorylation following cetuximab treatment

Twenty-one HNC tumor samples obtained prior to treatment with cetuximab (N=14) and/or following cetuximab therapy (N=7) were arrayed on a TMA and stained with an antibody directed against phospho-p70S6K (T421/S424). (A) The intensity of staining and the percentage of tumor cells that stained positively were determined and a composite score was calculated. The average composite score of pre-cetuximab and post-cetuximab tissues were graphed. (B) Expression of phospho-p70S6K in paired tissue (pre- and post-cetuximab treatment) from two HNC patients was assessed.

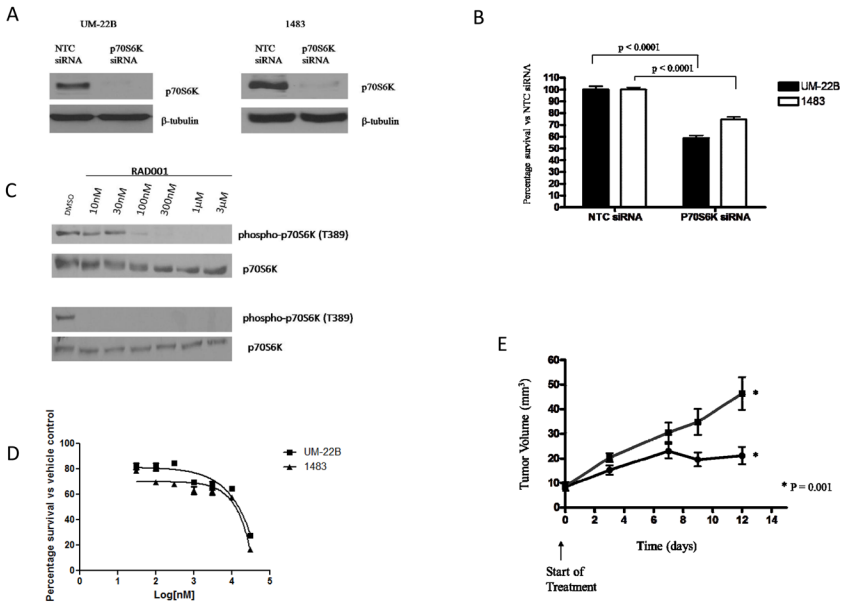

Figure 3. P70S6K targeting inhibits HNC cell growth

(A) HNC (UM-22B and 1483) cells were transiently transfected with p70S6K siRNA for 72 hours. Lysates were analyzed for p70S6K expression. β-tubulin was used as a loading control. (B) HNC (UM-22B and 1483 cells) were seeded in 24-well plates and transiently transfected with control (NTC) or p70S6K siRNA for 72 hours. MTT assay was performed and percentage survival was calculated. Percentage survival was graphed using GraphPad Prism Software. The experiment was performed twice with six replicates each ($P < 0.0001$). (C) 1483 (Top panel) and UM-22B (lower panel) cells were treated with various concentrations of RAD001 for 72 hours. Immunoblotting for phospho-p70S6K (Thr389) and p70S6K levels was performed. Figure is representative of 3 independent experiments. (D) 1483 and UM-22B cells were treated with different concentrations of RAD001 ranging from 30nM to 30μM for 72 hours. Cell-Titer Glo assay was performed and the IC_{50} survival curves were graphed with GraphPad prism Software. Figure is representative of 3 independent experiments. (E) HNC (UM-22B) cells were inoculated into the right flank of athymic nude mice and treated with placebo (■) or RAD001 (●) (5 mg/kg) daily by oral gavage. Tumors were measured 3 times weekly and the tumor volumes were calculated (10 mice per group; P=0.001).

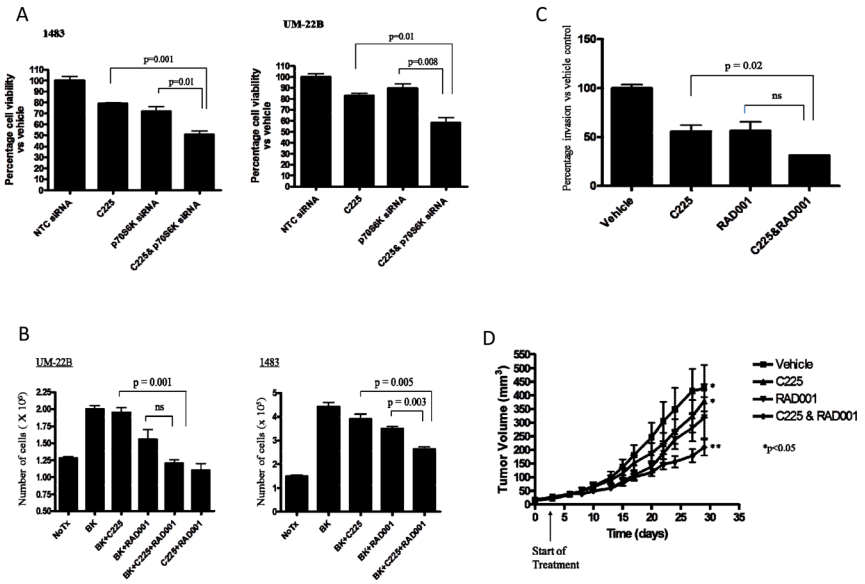

Figure 4. Combined targeting of EGFR and p70S6K results in enhanced anti-tumor efficacy

(A) HNC (1483 and UM-22B cells) were transfected with NTC or p70S6K siRNA. 24 hours later, siRNA-transfected cells were trypsinized, counted and seeded in 96-well plates. 24hours later, cells were treated with either vehicle or cetuximab (6μg/ml) for 24 hours. Cell-Titer Glo assay was performed according to manufacturer's instructions. Percentage survival was calculated and graphed using GraphPad Prism Software. The experiment was repeated twice in triplicate wells (1483, p=0.001, 0.01; UM-22B, p=0.01, p=0.008). (B) HNC (1483 and UM-22B) cells were treated with different combinations of BK (10nM), cetuximab (6 μg/ml), RAD001 (100 nM), alone or in combination. Cell growth was determined by trypan blue dye exclusion. The experiment was performed twice in triplicate with similar results (UM-22B, p=0.001;1483, p=0.005, 0.003). (C) 1483 cells were treated with cetuximab (6 μg/ml), RAD001 (100 nM), or a combination of C225 and RAD001 at the same concentration. Invaded cells were counted from 6 representative fields using light microscopy. The percentage invasion for each treatment was calculated and graphed. The difference between cetuximab and RAD001 alone versus combined treatment with cetuximab and RAD001 was determined (cetuximab vs cetuximab&RAD001, p=0.02). The experiment was performed 3 times with similar results. (D) HNC (1483) cells were inoculated in athymic nude mice, randomized into four treatment groups (10 mice per group); Vehicle (saline and 5 mg/kg placebo); cetuximab (0.8 mg twice weekly); RAD001 (5 mg/kg 5days/week); or cetuximab and RAD001 at the same doses. Tumors were measured 3 times weekly and tumor volumes were calculated (vehicle vs cetuximab & RAD001; P=0.0217, cetuximab vs cetuximab & RAD001; P=0.03). Data are shown as tumor volume ± SEM.

Table 1

Fold-increase in expression of phosphorylated proteins induced by PGE2 in EGFR siRNA- transfected cells compared to PGE2-stimulated control siRNA-transfected cells

Phospho-protein	Fold induction vs PGE2 stimulated NTC siRNA cells
Phospho-p70S6K	5.6
Phospho-PKCδ(Ser645)	3.6
Phospho-PKCθ (Ser676)	3.1
Phospho-IkBα (Ser32)	2.9
phospho-IRS1 (Ser312)	2.3
Phospho-MAPK (Thr202)	2.2

Table 2

Clinicopathologic characteristics of 19 patients evaluated for phosphorylated p70S6K

Gender, No. (%)	
Male	15 (79)
Female	4 (21)
Age, years	
Median (range)	64 (42–84)
Stage	
Locally advanced	5 (26)
Recurrent or metastatic	14 (74)
Primary site, No. (%)	
Oral cavity	8 (42)
Larynx	3 (16)
Oropharynx	4 (21)
Unknown primary	2 (11)
Other	2 (11)
Prior treatment, No. (%)	
Surgery	15 (79)
Radiotherapy	14 (74)
Chemotherapy	14 (74)
None	4 (21)
Cetuximab treatment	
Cetuximab alone	12 (63)
Cetuximab concurrently with radiotherapy	7 (37)